Feedback and Contact Information

Any questions or feedback may be forwarded to me at stephen.schneider@wpafb.af.mil or to Jeff Kemp at jeff.kemp@gtri.gatech.edu. If you wish to reference other previous AMTA publications, AMTA members can do so through our online archive at www.amta.org. If you are not a member, $75.00 and a few mouse clicks will get you registered as a member today! Both Jeff Kemp and I are open to feedback. Until next time!

Surface and Internal-Temperature Versus Incident-Field Measurements of Polyurethane-Based Absorbers in the Ku Band

Zhong Chen and Vince Rodriguez

ETS-Lindgren
1301 Arrow Point Drive, Cedar Park, Texas, 78613 USA
E-mail: zhong.chen@ets-lindgren.com, vince.rodriguez@ets-lindgren.com

Abstract

In recent years, there has been an increased need for testing antennas and radar systems at high power. Since absorbers work by transforming electromagnetic energy into thermal energy, there is a danger that in the presence of high fields, the absorber will reach temperatures that will cause it to ignite. In the present paper, standard polyurethane absorber was illuminated by a conical-horn antenna. Different field levels were used to illuminate the sample. The internal and surface temperatures of the sample were measured. From these measurements, the behavior of the temperature as a function of the field could be determined. Absorbers with and without a rubberized surface coating were also investigated to study their thermal behavior. This becomes very useful in determining if higher-power materials may be required for testing active arrays or radar systems. The effects of lowering the temperature of the absorber by using airflow across the tips were also studied.

1. Introduction

In the heating process of microwave absorbers under incident electromagnetic waves, two disciplines of physics are intertwined, i.e., the behavior of electromagnetic waves governed by Maxwell's equations, and the heat-transfer process dictated by laws of thermodynamics. The power density in the absorbers due to the electromagnetic field is given by

$$p = \sigma |E|^2 = 2\pi\varepsilon_0\varepsilon'' f |E|^2, \qquad (1)$$

where E is the total electric field (V/m) in the material, σ is the electrical conductivity of the material (S/m), ε_0 is the free-space permittivity (8.854×10^{-12} F/m), ε'' is the imaginary part of the relative dielectric constant, and f is the frequency in Hz. This is point form of Joule's law, and is well understood by RF engineers. The EM behavior of the polyurethane absorbers can be numerically computed. The EM field acts as the heating source, and its distribution in the absorber can provide a good indication of the locations of hot spots.

Polyurethane foam is an excellent insulator, so the conductive heat loss may be minimal. The heat exchanges can be reasonably described by radiation and convection transfers. Radiation takes place in the form of EM waves, mainly in the infrared region. The net power transferred from a body to the surroundings is described by Stefan-Boltzmann's law [1]:

$$p_{rad} = \varepsilon\sigma A\left(T^4 - T_0^4\right), \quad (2)$$

where A is the surface area, T is the surface temperature of the radiation body in K, and T_0 is the ambient temperature in K. Unfortunately, the conventional symbols used in heat transfer, σ and ε, are not the same as those in Equation (1). σ here is the emissivity or emission coefficient, and is defined as the ratio of the actual radiation emitted to the radiation that would be emitted from a black body. ε in Equation (2) is the Stefan-Boltzmann constant (5.67×10^{-8} W/m^{2}K^4). The context in the paper should make it clear to which symbols the authors are referring. Otherwise, we will make explicit references.

The convective heat transfer is due to the motion of air surrounding the absorbers. Two forms can take place, naturally or by forced air. The relationship is described by Newton's law of cooling [1]:

$$p_{conv} = hA\left(T - T_0\right), \quad (3)$$

where h is the convection heat-transfer coefficient in (W/m^{-2}K^{-1} W). h is often treated as a constant, although it can be a function of the temperature. Equation (3) assumes that the ambient air is abundant, and is taken to be constant. This is a reasonable assumption, because the heating is typically confined to a small localized area in a relatively large anechoic chamber. Combining the two mechanisms of heat transfer, the total heat loss is given by

$$p = \varepsilon\sigma A\left(T^4 - T_0^4\right) + hA\left(T - T_0\right). \quad (4)$$

It is possible to solve for the temperatures from coupled Maxwell's and heat-transfer equations. Realistic results require accurate electrical and thermal properties of the materials. It is often a nontrivial process to obtain the material properties in and of itself. Careful validation is warranted before we can have full confidence in the results. In this paper, we instead adopt a measurement approach. We conducted a series of experiments to measure the temperature both on the surface of the absorbers, using an infrared imaging camera, and internally, using thermocouple probes inserted into the absorbers. Temperature profiles as functions of the applied E field were experimentally established. From the measured data, we curve fitted to Equation (4) or other mathematical functions. These functions were useful for calculating results at other field levels, e.g., extrapolating to a higher field, where measurement results cannot be readily obtained.

2. Field Distribution Inside the Absorbers

Numerical analysis was performed using Ansys *HFSS*, a commercially available finite-element software package. As was described in [2], symmetry was taken advantage of, so only one-quarter of the pyramidal absorber was solved. The quarter pyramid was located inside a square-cross-section prism that bounded the computational domain. The structure was fed using a port located on the top of the geometry, and the side boundaries of the domain were set as perfect electric conductors (PEC) or perfect magnetic conductors (PMC). The base was modeled as PEC. This was exactly the same approach taken in [2]. The structure of a CRV-23PCL-4 was analyzed at 12.4 GHz, the same frequency used in the measurements. The resulting field was extracted at one plane. The plane was one of the two orthogonal planes that cut the pyramid into four sections. Figure 1 shows the field distribution at 12.4 GHz. The curvature of the absorber profile was added for clarity. The results were an approximation. The permittivity of the material was assumed to be fairly constant from 6 GHz to 12 GHz. The purpose of the numerical analysis was to check the expected field distribution in the pyramid, which we could use to compare with the infrared (IR) images of the absorbers taken during the measurements.

The field-distribution data showed that most of the field existed on the upper third of the pyramid. It also showed that there was a region of high field existing in the valleys between the pyramids. The surface-temperature profile from the IR pictures showed that this was a real phenomenon. On the other hand, the field was higher at the very tip of the absorber. Measurements from the IR images seemed to contradict this result. This could be explained. Since the tip was smaller, it cooled faster to the surrounding ambient temperature.

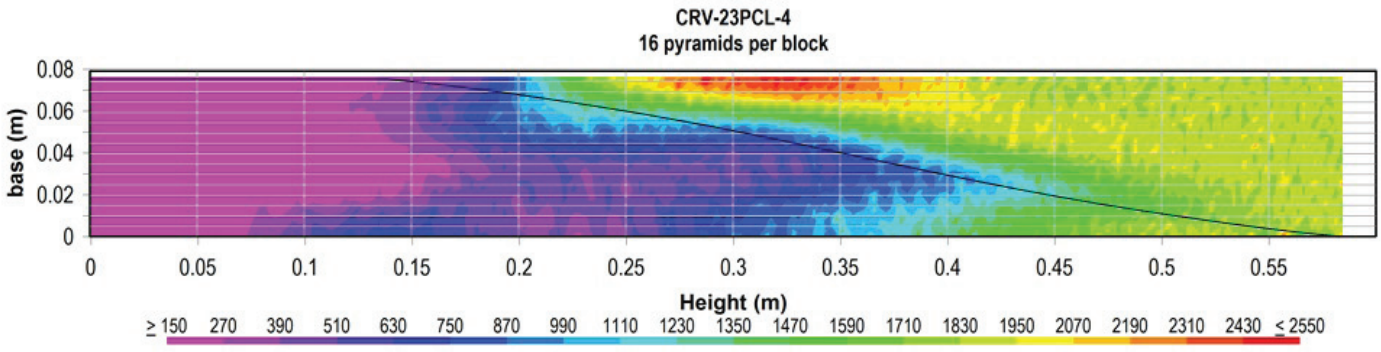

Figure 1. The electric field distribution at 12.4 GHz.

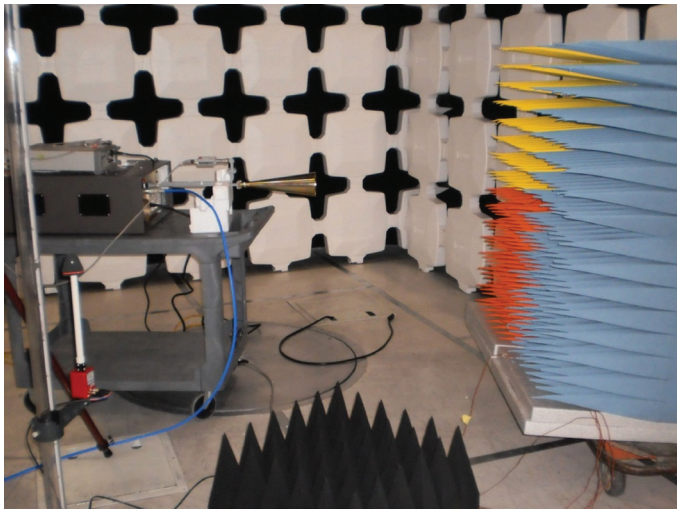

Figure 2. The test setup, using a conical-horn antenna to illuminate the absorbers.

3. Experimental Setup and Data

Experiments were performed on ETS-Lindgren CRV-23PCL-8 and CRV-23PCL-4 absorbers at 12.4 GHz. Both types were 23 in long from tips to bases. A piece had a base size of 2 ft × 2 ft. A CRV-23PCL-8 piece consisted of $8 \times 8 = 64$ pyramids, whereas a CRV-23PCL-4 piece consisted of $4 \times 4 = 16$ pyramids. The two types were designed to have similar RF performance, but the CRV-23PCL-8 was made of slender pyramids to facilitate better heat transfer to the surroundings [2]. The absorbers were mounted on particle board with metallic backings, and were placed in front a Ku-band horn antenna with a circular aperture (the gain was approximately 20 dBi). A 300 W amplifier was used, and the power to the antenna was monitored through a 40 dB directional coupler connected to a power meter. The test setup is shown in Figure 2. The ambient temperature was at 23°C.

As a first step, a 200 V/m field was generated by leveling to a calibrated electric-field probe. The distance from the probe to the antenna was 30 in. At this distance, near-field coupling was assumed to be negligible, and the incident wave was assumed to be uniform (numerical simulation also validated these assumptions). The power needed to generate the 200 V/m field was recorded. The field probe was next replaced with the absorbers under test. The tips of the absorbers were placed at the same distance (30 in) from the antenna. Other field strengths could be leveled by scaling from the power for 200 V/m.

3.1 Surface Temperature

Figures 3 and 4 show two examples of the infrared images taken after the temperature reached equilibrium under continuous-wave constant fields of 400 V/m, 700 V/m, and 800 V/m at $f = 12.4$ GHz for the two types of absorbers described earlier. There was no forced airflow during the measurement. Table 1 summarizes the resulting temperatures on the absorber surfaces at different field levels. Tests were performed on two finishes of otherwise identical CRV-23PCL-8 absorbers, i.e., fully covered with rubberized paint, or with latex paint. The data indicated that the paint had minimal effect on absorber temperatures. Table 1 also lists data for the wider CRV-23PCL-4 absorbers (with latex paint).

3.2 Internal Temperature of the Absorber Recorded by Thermocouples

Three thermocouples were inserted in the CRV-23PCL-8, which were painted with rubberized coating. They were inserted at distances of 4 in, 6 in, and 8 in from the tip of the pyramid, as illustrated in Figure 5. Figure 6 shows the temperatures measured by the three sensors. The temperatures at 8 in from the tip were consistently higher than at other locations. There

Table 1. The maximum surface temperature recorded by the IR camera (at equilibrium), $T_0 = 23°C$.

E (V/m)	Power Density (kw/m^2)	CRV-23PCL-8 Rubberized (°C)	CRV-23PCL-8 Latex (°C)	CRV-23PCL-4 Rubberized (°C)
200	0.11	24	–	–
300	0.24	–	–	28
360	0.34	30	–	–
400	0.42	35	36	43
500	0.66	41	–	50
600	0.95	54	–	67
700	1.30	63	–	82
800	1.70	72	73	93
950	–	–	–	112

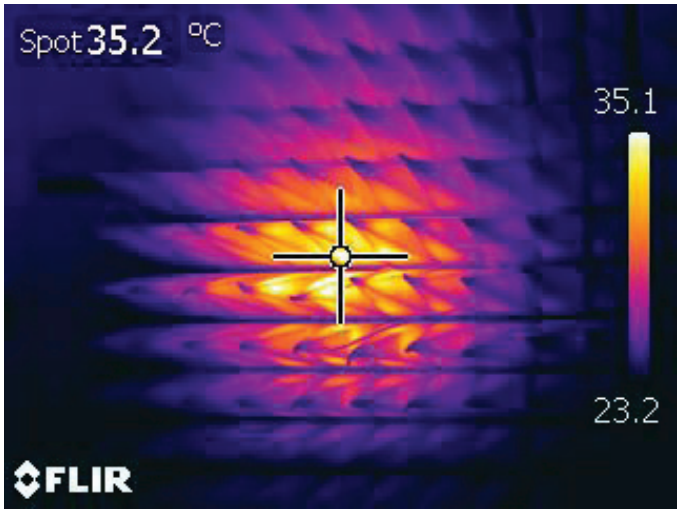

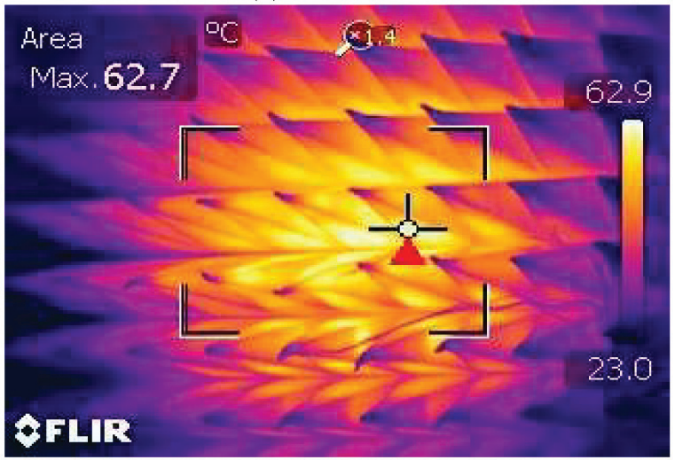

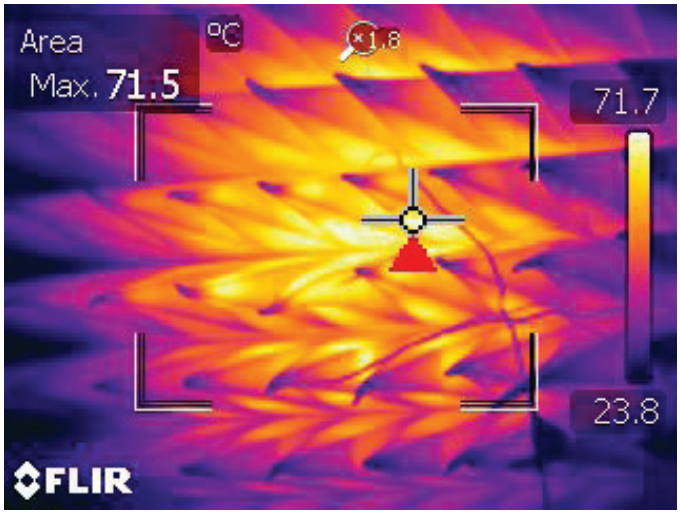

Figure 3. Infrared camera images for incident electric fields of (a, top) 400 V/m, (b, middle) 700 V/m, and (c, bottom) 800 V/m. The absorber was the slender CRV-23PCL-8.

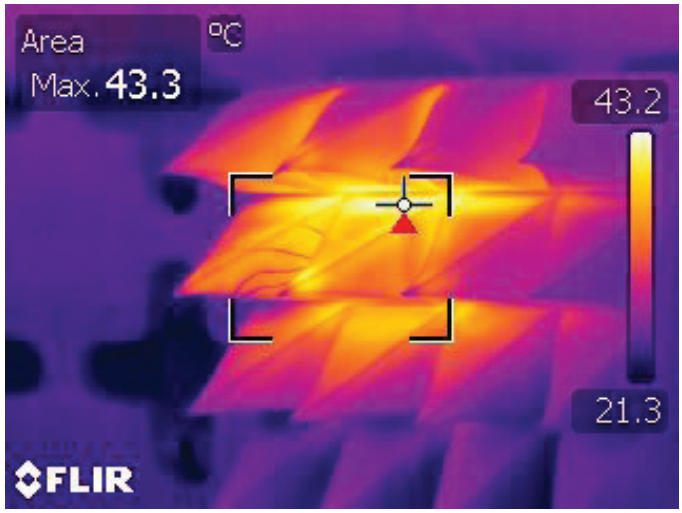

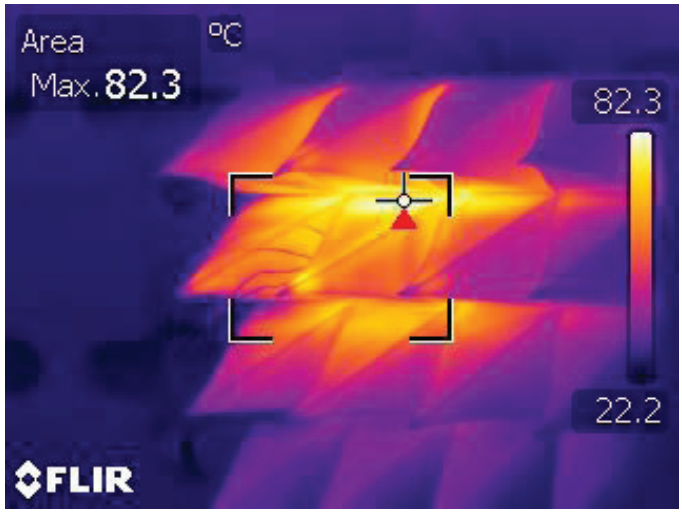

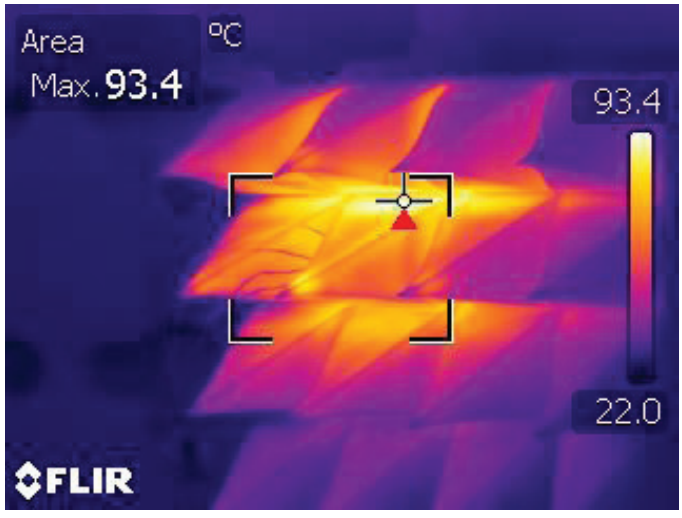

Figure 4. Infrared camera images for incident electric fields of (a, top) 400 V/m, (b, middle) 700 V/m, and (c, bottom) 800 V/m. The absorber was the wider CRV-23PCL-4.

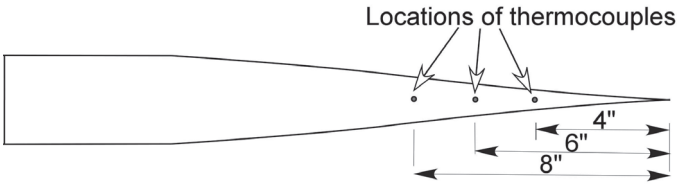

Figure 5. The locations of the thermocouple sensors. The sensors were inserted halfway into the middle of the absorber pyramid.

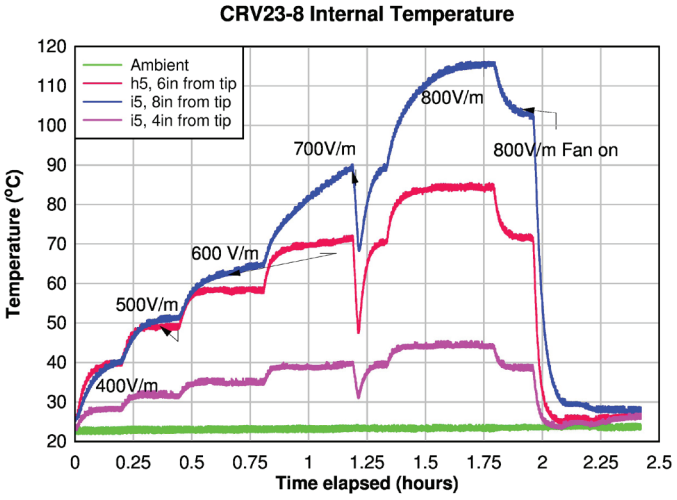

Figure 6. The temperatures inside the CRV-23PCL-8 absorbers as measured by the thermocouples.

was a gap in the data at 700 V/m because RF power was briefly turned off. The internal temperature reached 115°C under 1.7 $\mathrm{kW/m^2}$ (800 V/m). Since the maximum allowed temperature for the polyurethane foam material was 125°C, it is recommended that the incident power density remain less than 1.7 $\mathrm{kW/m^2}$ for CRV-23PCL-8 absorbers mounted vertically and with natural convection in a 23°C room.

After the temperature reached equilibrium under 800 V/m, additional airflow was introduced by turning on a 6 in diameter fan at 45 in in front of the absorbers. The airflow rate was measured to be approximately 80 ft/min at this distance. Note that this was a rather moderate airflow, which could arise naturally from air-conditioning vents in a chamber. As shown in Figure 6, the internal temperature quickly dropped to 102°C from 115°C.

There was no visual change to the absorbers, nor were there noticeable odors during or after the entire test.

4. Data Analysis

4.1 Surface Temperature

The surface temperature as a function of the power is described by Equation (4), or this can be rewritten as

$$p = \left(E^2/120\pi\right)A = k_1\sigma\left(T^4 - T_0^4\right) + k_2\left(T - T_0\right), \quad (5)$$

where E is the field strength (V/m) of the incident plane wave, and A is the area ($\mathrm{m^2}$) of illumination. Since A is a constant, it can be dropped or merged into constants k_1 and k_2. The two unknown coefficients, k_1 and k_2, in Equation (5) are determined through a least-squares curve fit to the measured data. For the CRV-23PCL-8 with rubberized coating (Table 1, column 3),

$$k_1 = 0.6678,$$

$$k_2 = 27.93.$$

A simple second-order polynomial fit is also shown in Figure 7. The second-order polynomial fit yielded a response similar to the model given by Equation (5). From Equation (5), the ratio of the radiation to the combined radiation and convection heat loss could be solved for. Figure 8 shows the ratio of heat loss due to radiation. It was interesting to note that the radiation heat loss constituted a small but significant percentage of the total heat loss (approximately 15%).

From Table 1, it could be seen that the rubberized coating on the absorber had no impact on the temperature and the heat transfer (comparing columns 3 and 4). The maximum surface temperatures of CRV-23PCL-8 with and without rubberized paint showed almost identical results.

Table 1 also showed that the slender design of CRV-23PCL-8 exhibited lower temperatures under the same incident field as compared to the wider CRV-23PCL-4. The slender design indeed improved the power-handling capability [2]. The results are seen in Figure 9.

4.2 Internal Temperature

Radiation heat transfer was insignificant inside the absorbers. For temperatures in the absorbers, we could assume the

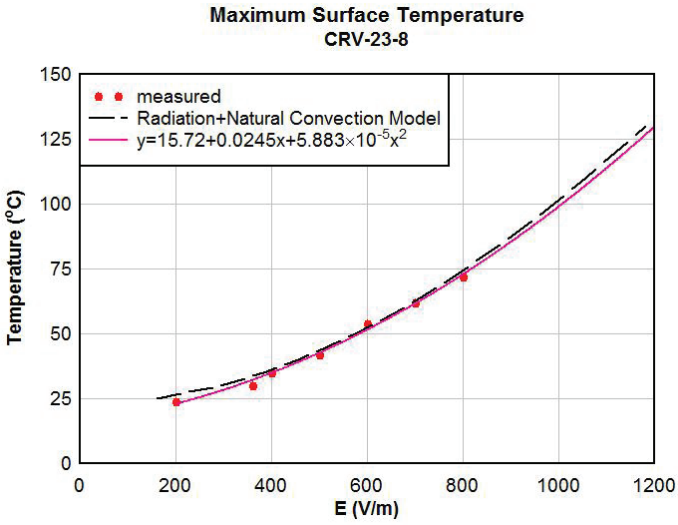

Figure 7. The maximum surface temperature as a function of the incident electric field for CRV-23PCL-8 with rubberized paint. The chart shows the measured data, the data curve-fitted to the heat-transfer equation, and a second-order polynomial curve fit.

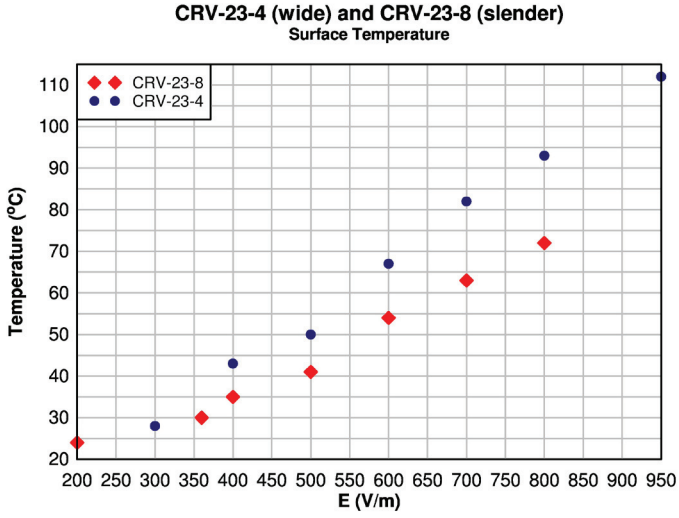

Figure 9. The maximum surface temperature of the slender CRV-23PCL-8 and the wider CRV-23PCL-4.

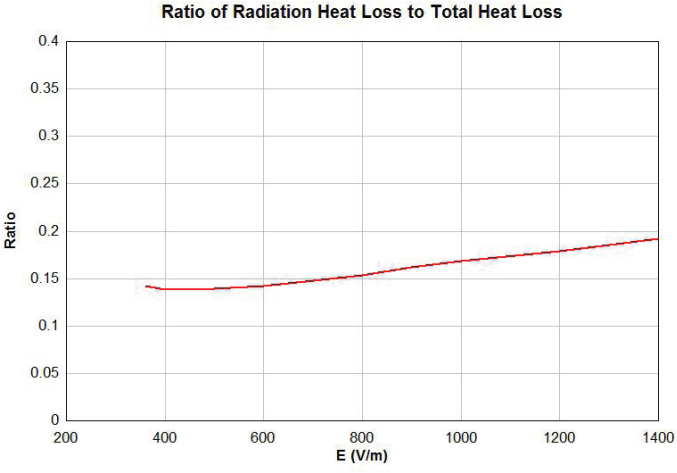

Figure 8. The ratio of the heat loss due to radiation to the total heat loss.

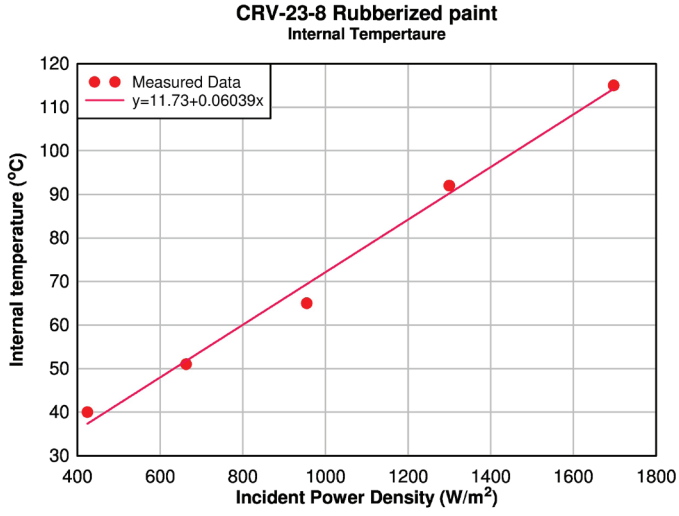

Figure 10. The maximum internal temperature measured by thermocouples as a function of the incident power density.

incident power was linearly proportional to the temperature, i.e.,

$$p = k\left(T - T_0\right), \tag{6}$$

where k is a constant. Figure 10 shows the internal temperatures inside the CRV-23PCL-8 absorbers measured by thermocouples at the 8 in position, as it measured the maximum internal temperature. Figure 10 also shows a linear fit to the measured data. The linear model proved to be a reasonable assumption.

5. Summary

Measured temperature data was presented for polyurethane absorbers under varying field strengths at 12.4 GHz, both on the surface and inside the absorbers. Mathematical models were validated, based on the underlying heat-transfer mechanisms. The coefficients of the models could be solved for from curve fitting to the measured data. The models are useful for "predicting" absorber temperatures under otherwise difficult-to-achieve field levels. Absorbers with slender profiles proved to have improved power-handling capabilities. Applying forced air at a relatively low flow rate can significantly decrease the absorbers' temperatures. In addition, rubberized paint on the absorber's surface does not have a noticeable effect on the temperature of the absorbers.

6. Acknowledgment

The authors wish to thank Sergio Longoria, Doug Kramer, Chris Carpenter, and Garth D'Abreu of ETS-Lindgren for their help during the measurements.

7. References

1. Theodore L. Bergman, Adrienne S. Lavine, Frank P. Incropera, and David P. DeWitt, *Fundamentals of Heat and Mass Transfer, Sixth Edition*, New York, John Wiley & Sons, 2006.

2. V. Rodriguez, G. D'Abreu, and K. Liu, "Measurements of Power Handling of RF Absorber Materials: Creation of a Medium Power Absorber by Mechanical Means," Proceedings of the 31st Annual Symposium of the Antenna Measurement Techniques Association, AMTA2009, Salt lake City, UT, November 2009.